

RESEARCH ARTICLE

10.1002/2017JC012840

Distribution of Upper Circumpolar Deep Water on the warming continental shelf of the West Antarctic Peninsula

Nicole Couto¹ , Douglas G. Martinson² , Josh Kohut¹ , and Oscar Schofield¹ 

Key Points:

- Autonomous underwater vehicles provide measurements of mesoscale features (~10 km) in the Antarctic with high-spatial resolution
- Mesoscale eddy-like features contribute significantly to the heat budget of the west Antarctic Peninsula continental shelf
- Upper Circumpolar Deep Water consistently intrudes onto the WAP shelf in bathymetric depressions

Correspondence to:

N. Couto,
ncouto@marine.rutgers.edu

Citation:

Couto, N., D. G. Martinson, J. Kohut, and O. Schofield (2017), Distribution of Upper Circumpolar Deep Water on the warming continental shelf of the West Antarctic Peninsula, *J. Geophys. Res. Oceans*, 122, doi:10.1002/2017JC012840.

Received 28 FEB 2017

Accepted 31 MAY 2017

Accepted article online 5 JUN 2017

¹Department of Marine and Coastal Sciences, Rutgers University, New Brunswick, New Jersey, USA, ²Lamont-Doherty Earth Observatory, Columbia University, Palisades, New York, USA

Abstract We use autonomous underwater vehicles to characterize the spatial distribution of Upper Circumpolar Deep Water (UCDW) on the continental shelf of the West Antarctic Peninsula (WAP) and present the first near-synoptic measurements of mesoscale features (eddies) containing UCDW on the WAP. Thirty-three subsurface eddies with widths on the order of 10 km were detected during four glider deployments. Each eddy contributed an average of 5.8×10^{16} J to the subpycnocline waters, where a cross-shelf heat flux of 1.37×10^{19} J yr⁻¹ is required to balance the diffusive loss of heat to overlying winter water and to the near-coastal waters. Approximately two-thirds of the heat coming onto the shelf diffuses across the pycnocline and one-third diffuses to the coastal waters; long-term warming of the subpycnocline waters is a small residual of this balance. Sixty percent of the profiles that contained UCDW were part of a coherent eddy. Between 20% and 53% of the lateral onshore heat flux to the WAP can be attributed to eddies entering Marguerite Trough, a feature in the southern part of the shelf which is known to be an important conduit for UCDW. A northern trough is identified as additional important location for eddy intrusion.

1. Introduction

Most of the glaciers along the West Antarctic Peninsula (WAP) have retreated since the early 1950s [Cook *et al.*, 2005], and the rate at which ice sheets have been losing mass has accelerated over the past decade [Rignot *et al.*, 2014]. The glacial retreat has been attributed to calving events, linked to warming atmospheric temperatures, and melting from below, attributed to the onshore transport of warmer ocean water [Rignot and Jacobs, 2002; Jenkins *et al.*, 2010; Pritchard *et al.*, 2012; Cook *et al.*, 2016]. Atmospheric temperatures over the WAP have warmed at an approximate rate of 0.5°C per decade since the 1950s [Meredith and King, 2005; Turner *et al.*, 2006; Bromwich *et al.*, 2013], although recent observations show a reversal of the warming trend since the late 1990s, consistent with the large variability of the system [Turner *et al.*, 2016]. Summertime upper ocean water temperatures rose by more than 1°C between the mid-1950s and mid-1990s [Meredith and King, 2005] and continued to increase at a rate of 0.1–0.3°C per decade since the 1990s [Schmidtke *et al.*, 2014]. This warming reflects the effects of changes in atmospheric temperatures. Recent observations, however, suggest that glacier retreat on the WAP is driven primarily by deep ocean temperatures [Cook *et al.*, 2016] which can also supply heat to the atmosphere [Venables *et al.*, 2016].

Upper Circumpolar Deep Water (UCDW) is the largest source of ocean heat to the WAP continental shelf [Hofmann *et al.*, 1996]. This water mass is characterized by potential temperatures exceeding 1.7°C and salinities greater than 34.54 [Martinson *et al.*, 2008], and is the warmest deep water mass observed on the WAP continental shelf. UCDW is found just off the shelf at depths between 200 and 600 m within the Antarctic Circumpolar Current (ACC), an eastward-flowing current that runs directly along the continental slope of the WAP [Klinck, 1998; Klinck *et al.*, 2004]. While surface water properties on the continental shelf vary seasonally with the growth and melting of sea ice and variable wind mixing [Hofmann *et al.*, 1996], water below the permanent pycnocline is kept warm throughout the year by frequent intrusions of UCDW from the offshore ACC [Smith *et al.*, 1999; Martinson *et al.*, 2008].

Overlying the relatively warm deep water on the shelf is Winter Water. This cold water mass is generated from a combination of sea ice growth, sensible heat loss to the atmosphere, and deep vertical mixing driven by winds during the winter and is persistent in most parts of the shelf throughout the summer. In the

winter, it extends from the surface to around 200 m. Beginning in the spring, relatively fresh sea ice meltwater creates a shallow surface layer that overlies the Winter Water and warms throughout the summer. As UCDW intrudes onto the shelf, it loses heat to the surrounding water and overlying Winter Water through both diapycnal and isopycnal mixing [Smith *et al.*, 1999]. Over the course of the year on the continental shelf, there is a net flux of heat out of the surface ocean with a magnitude estimated between 6 W m^{-2} (using data from 1993 only) [Smith and Klinck, 2002] and 19 W m^{-2} (averaged over 1993–2004) [Martinson *et al.*, 2008]. The cross-pycnocline heat flux from UCDW-warmed water into the Winter Water balances this heat loss to the atmosphere. The temperature gradient that drives this vertical diffusion of heat is preserved by subpycnocline along-isopycnal heat transport from off the shelf [Klinck *et al.*, 2004].

Several mechanisms have been suggested for delivering UCDW to the WAP. Upwelling of offshore UCDW is evidenced in hydrographic data by shoaling of the permanent pycnocline [Martinson *et al.*, 2008]. Topographically induced or wind-driven upwelling events have been linked to large diatom blooms on the shelf [Prézelin *et al.*, 2000]. However, shoaling may not always indicate upwelling; it can also be produced when a subsurface eddy moves onto the shelf and deflects isopycnals [Martinson and McKee, 2012]. Indeed, with the high-temporal resolution of mooring observations in Marguerite Trough and the neighboring shelf, and the increased spatial resolution of regional models, mesoscale eddies have emerged as the most prominent mechanism of heat delivery to the WAP shelf [Dinniman *et al.*, 2011; Martinson and McKee, 2012]. While upwelling has not been ruled out as a potential delivery mechanism [Martinson and McKee, 2012], the apparent shelf-wide flooding of UCDW documented in coarsely resolved hydrographic surveys [Prézelin *et al.*, 2004] was shown to actually be the result of coherent eddies moving on to the shelf and dissipating heat [Moffat *et al.*, 2009; Dinniman *et al.*, 2011; Martinson and McKee, 2012].

Eddies are carried onto the shelf during episodic advective intrusions of UCDW, which may occur during periods of intense wind stress [Dinniman *et al.*, 2011]. Modeling studies and observations indicate that, with a strong enough forcing, when the mean shelf break flow encounters curving bathymetry, some of the water flowing in the ACC along the shelf break is carried by momentum onto the shelf [Dinniman and Klinck, 2004; Klinck *et al.*, 2004]. Evidence from a high-resolution model also suggests that Rossby waves at the shelf break can interact with a trough to produce features consistent with eddies [St-Laurent *et al.*, 2013].

Moorings in Marguerite Trough and on the surrounding shelf have recorded eddies passing by at rates of three to four per month [Moffat *et al.*, 2009; Martinson and McKee, 2012], but presence elsewhere on the shelf is largely unknown. Existing data sets in the region were collected using traditional shipboard sampling, with measurements typically made at coarser resolution than that required to resolve mesoscale eddies on the WAP. Weak subsurface stratification of the shelf combined with the effects of high-latitude result in a small radius of deformation which determines the length scale of eddy dynamics [Chelton *et al.*, 1998]. Eddies shed from the ACC have diameters of $\sim 10\text{--}20 \text{ km}$ [Klinck and Dinniman, 2010].

Here we use data from four deployments of Slocum-Webb autonomous underwater vehicles (gliders) to map the spatial distribution of UCDW on the shelf. Some of the UCDW is contained in subsurface mesoscale eddies with widths on the order of 10 km. Glider profiles are 1 km apart, on average, providing sufficient spatial resolution to define the horizontal boundaries of mesoscale features. These data allow us to identify previously undetected pathways of intrusion for eddies onto the shelf, and allow us to estimate their relative importance to the WAP continental shelf heat budget.

We place these glider deployments in the context of annual shelf-wide hydrographic data from repeat cruises conducted each January from 1993 to 2008 [Smith *et al.*, 1995; Ducklow *et al.*, 2012]. Hydrographic stations occupied during these cruises were rarely closer than 20 km apart, so they lack the spatial resolution to detect eddies on the shelf, but they allow us to construct a subpycnocline heat budget from which we can estimate the contribution of subsurface eddies carrying UCDW and discuss their impact on the warming trend observed across the shelf over the last several decades.

2. Methods

This study uses data obtained from four deployments of Slocum Webb deep gliders from Palmer Station, Antarctica ($64^{\circ}46'S$, $64^{\circ}03'W$) during austral summers 2010–2011, 2011–2012, and 2012–2013. Deployments lasted between 29 and 62 days and covered distances up to 1600 km in the coastal waters west of the

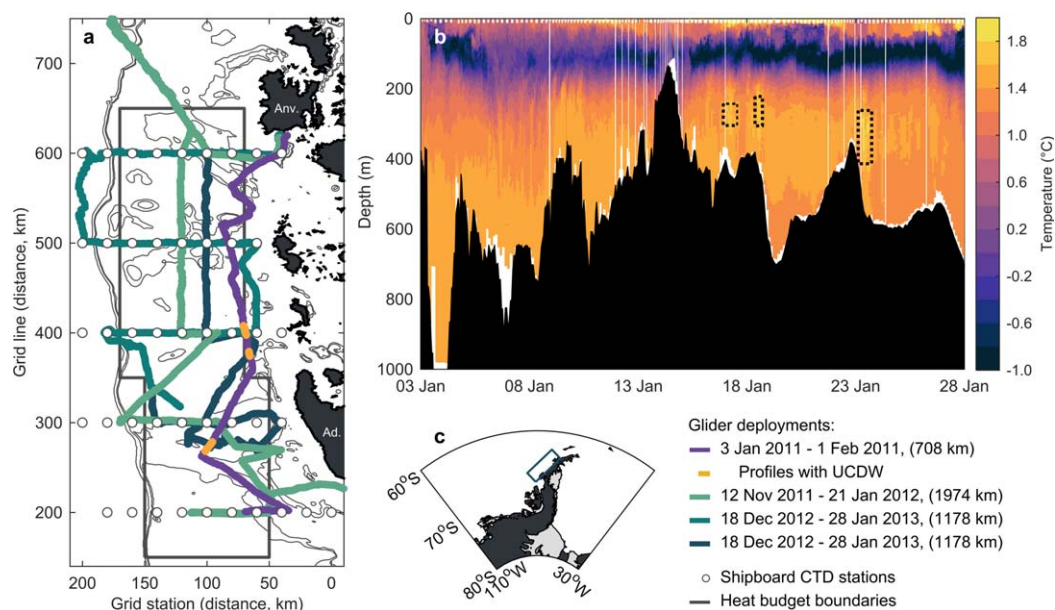


Figure 1. (a) The region of the WAP continental shelf discussed in this analysis. Shipboard CTD profile locations used in the heat budget calculations are shown as circles. The gray box encloses stations used to calculate the change in shelf heat over time and the vertical heat flux to the winter water layer. Lateral diffusion is measured across the right box boundary and lateral onshore heat flux is calculated across the left box boundary. Green and purple lines show tracks of the four glider deployments. Temperature data from the purple track are shown in Figure 1b with yellow dots indicating profiles where UCDW was found. Bathymetry contours are plotted at the 500, 600, and 1000 m isobaths. Anvers (Anv.) and Adelaide (Ad.) Islands are labeled. (b) Temperature section from the glider deployment shown in purple in Figure 1a. Dotted boxes show the extent of UCDW in the three mesoscale features detected on this deployment. (c) Regional map, with boundaries of plot a shown.

Antarctica Peninsula (Figure 1). Gliders are buoyancy-driven autonomous underwater vehicles that move from the surface to a depth of up to 1000 m with an average horizontal speed of 1 km h^{-1} [Davis *et al.*, 2002; Schofield *et al.*, 2007]. All gliders used in this study were equipped with a Seabird CTD to measure conductivity, temperature, and depth with a sampling resolution of 4–6 measurements per vertical meter. Data from each dive or climb were averaged into 1 m depth bins and the latitude/longitude of the entire profile was set to the average latitude/longitude of the climb or dive.

In each of the four deployments, gliders traveled generally southward along the peninsula. We restrict our focus to profiles taken on the continental shelf, which we define as shoreward of the 600 m isobath (Figure 1a). Among the shelf profiles, UCDW ($T > 1.7^\circ\text{C}$ and $S > 34.54$, Martinson *et al.* [2008]) was often encountered below the permanent pycnocline as part of distinct boluses with characteristics consistent with subsurface eddies (Figure 1b).

Studies of subsurface eddies in the North Pacific [Pelland *et al.*, 2013] and North Atlantic [Bower *et al.*, 2013] suggest that a Gaussian distribution model is appropriate for defining the horizontal boundaries of those features. We use it to measure chord lengths of the eddy-like boluses encountered by the gliders. From here forward, we will refer to the boluses as “eddies.” The model assumes that the cross section of an eddy along an isopycnal is circular and that its temperature is greatest at its center and decays in the radial direction. This geometry is described by the following equation:

$$T' = T_{\max} \cdot e^{-\left(\frac{x-x_0}{r}\right)^2}, \quad (1)$$

where T' is the temperature anomaly at position x , T_{\max} is the maximum value of the anomaly at the eddy center, x_0 , and r is the eddy radius.

Following the methods of Zhang *et al.* [2015], who calculated widths of subthermocline eddies in the North Pacific using Argo float profiles, we interpolated temperature profiles onto surfaces of constant potential density separated by 0.01 kg m^{-3} . For each isopycnal surface, using only observations on the shelf, we calculated the mean temperature and anomalies from the mean. We then identified every shelf profile that

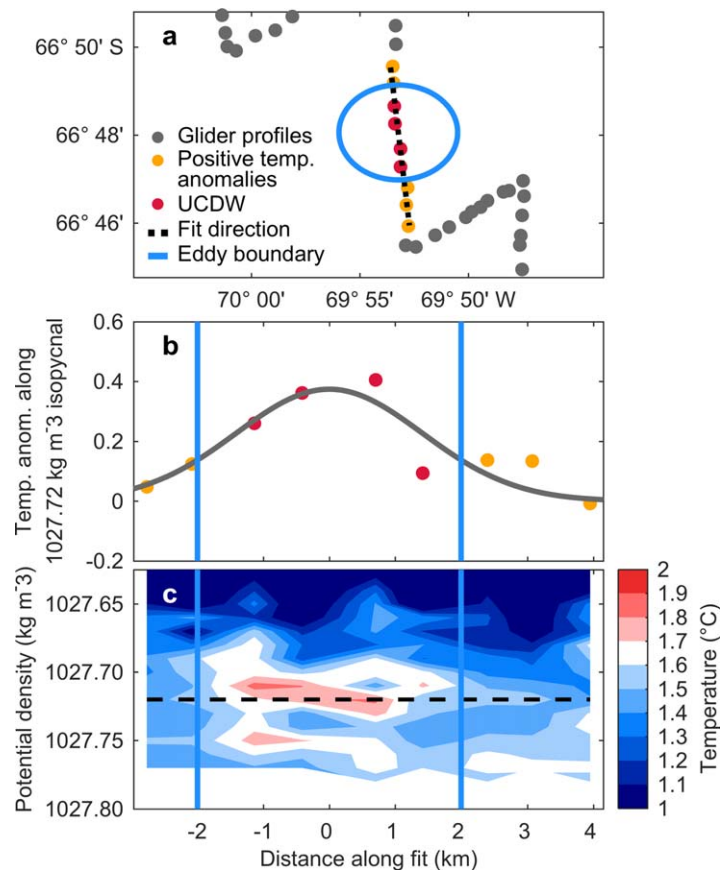


Figure 2. Example of method used to define eddy width. (a) Profiles containing UCDW at any depth are identified based on temperature and salinity values (red dots). One isopycnal surface is selected and the surrounding profiles that contain positive temperature anomalies along that surface are identified (yellow dots). A least-squares line is fit to these profiles (black dashed line). (b) A Gaussian curve is fit to the positive temperature anomalies along the chosen isopycnal in the direction of the least squares fit. Eddy width is defined by equation (1) as twice the radius, enclosing 84.3% of the heat (vertical blue lines). (c) Temperature section with vertical blue lines showing the calculated eddy width. Dots in Figures 2a and 2b show the locations of each glider profile (a single dive or climb).

contained UCDW at any depth and fit Gaussian curves to the positive temperature anomalies surrounding these profiles on each of fifteen isopycnal surfaces between $1027.63 \text{ kg m}^{-3}$ (approximating the base of the winter mixed layer and the shallowest isopycnal where UCDW was found) and $1027.77 \text{ kg m}^{-3}$ (the deepest isopycnal that at least 50% of glider profiles extended to).

We used the MATLAB “fit” function to calculate the radii of the eddies according to equation (1) (Figure 2). Distances (x) were measured along the least squares fit line through all points on the isopycnal surrounding the UCDW profile that had positive temperature anomalies (Figure 2a). This method was repeated for every profile containing UCDW and every potential density surface between 1027.63 and $1027.77 \text{ kg m}^{-3}$, resulting in several fits to the same feature; we chose the best as the fit with the lowest rms/mean. Isopycnals representing the best fits ranged from 1027.70 to $1027.76 \text{ kg m}^{-3}$.

Eddy chord lengths were defined according to equation (1) as twice the radius, r , which encloses 84.3% of the temperature anomaly in the fit (Figure 2b). These lengths are used as an estimate for eddy width, but since we do not know how closely the glider passed through eddy centers, nor do we know the direction of eddy movement, there is error in this estimate. Drawing random lines through a stationary circle to measure the diameter would result in an average estimate that is 68% of the true diameter, but eddies are not assumed to be stationary during the time the glider spent sampling them. Width is likely to have been underestimated (overestimated) during times when the glider passed through an eddy as it was carried by the mean flow in the opposite (same) direction as the glider motion.

The heat content of each eddy was calculated relative to the average shelf temperature, T_{ref} .

$$Q = \int_{z_1}^{z_2} (T - T_{ref}) \rho_z c_p \pi r^2 dz, \quad (2)$$

where z_1 and z_2 are the shallowest and deepest depths where UCDW was observed within a single eddy. These depths averaged 221 and 346 m on the shelf across all glider deployments. The reference temperature, T_{ref} , was calculated as the average potential temperature below the permanent pycnocline of all non-UCDW profiles on the shelf and had a value of 1.2°C . Since the reference temperature includes every profile where the maximum potential temperature was below 1.7°C and does not demand that the profile be cooled any further, heat calculated relative to this temperature represents a lower bound of the heat delivered to the shelf by eddies.

Temperature profiles were also taken during annual cruises in January 1993 and 1995–2015 as part of the Palmer Long Term Ecological Research (LTER) project. The LTER grid is made up of lines running along the peninsula spaced 100 km apart and stations running perpendicular to the shelf spaced 20 km apart (Figure 1a). The lines are named according to distance from a point south of this particular study area: the 200 line extends out from south of Adelaide Island and, 400 km northeast of that, the 600 line extends out from south of Anvers Island (Figure 1). The same temperature and salinity criteria ($T \geq 1.7^\circ\text{C}$, $S \geq 34.54$) used to identify UCDW in the glider data were used to identify UCDW in the shipboard CTD data, and the same potential density surfaces were used to calculate the heat content of every profile. These data were used to investigate the spatial patterns of UCDW on the shelf. They were also used to create a volume-averaged heat budget for the WAP shelf in order to determine the importance of the subsurface eddies as a source of heat to the shelf.

3. Results and Discussion

3.1. Locations of UCDW Intrusions

Hydrographic measurements on the WAP, taken from both traditional ship platforms and glider deployments, reveal a consistent pattern of intrusion locations onto the shelf (Figure 3). Both data sets show a heightened presence of UCDW on the shelf in deep areas, mostly confined to the region around Marguerite Trough (300 and 400 lines). In both data sets, observations of UCDW drop off with distance from the shelf break toward the coast, as expected, since processes on the shelf lead to the modification of UCDW.

Ocean gliders have significantly improved the spatial resolution of hydrographic measurements along the Antarctic Peninsula, allowing us to resolve features smaller than the spacing of a typical ship-based survey [Heywood *et al.*, 2014; Erickson *et al.*, 2016]. The increased sampling resolution of the gliders increases the likelihood of encountering the small-scale features containing UCDW. The glider data confirm our understanding of UCDW intrusion locations but indicate that studies based solely on hydrographic surveys with profiles separated by 20 km or more have underestimated the quantity of unmixed UCDW on the shelf (Figure 3, blue bars versus red bars). During some LTER cruises, no UCDW was seen on the shelf, but it easily could have been missed; a single CTD cast from a ship is meant to represent a 20 km × 100 km area of ocean, within which it is possible for several mesoscale features to exist but go undetected. Glider surveys consistently encountered more UCDW per unit effort (profiles measured) than did shipboard surveys.

The glider data allow us to separate UCDW that appears in coherent eddies from UCDW present outside eddy-like structures. Coherent features carrying UCDW were seen in each of the four glider deployments. Of all profiles containing UCDW, 60% occurred as part of eddies (Figure 3, pink bars versus red bars). The UCDW found outside of eddies was present either near the shelf break spread over tens of kilometers, which may be evidence of a mean advection across the shelf break,

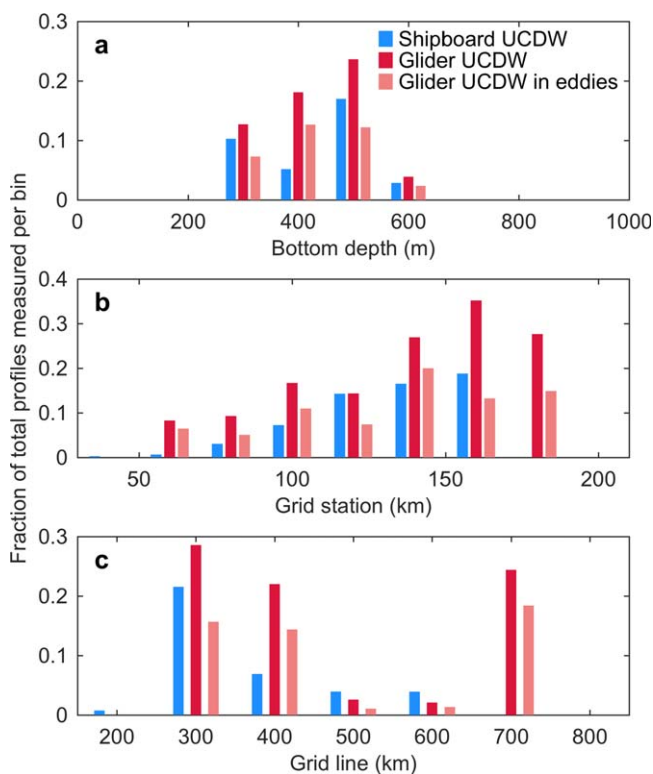


Figure 3. Fractions of (blue) total shipboard CTD profiles that contained UCDW, (red) total glider CTD profiles that contained UCDW, and (pink) total glider CTD profiles that were part of an eddy, that were found in bins of (a) bottom depth, (b) grid station, and (c) grid line. Eddy profiles were identified by fitting Gaussian curves to temperature anomalies, as described in section 2.

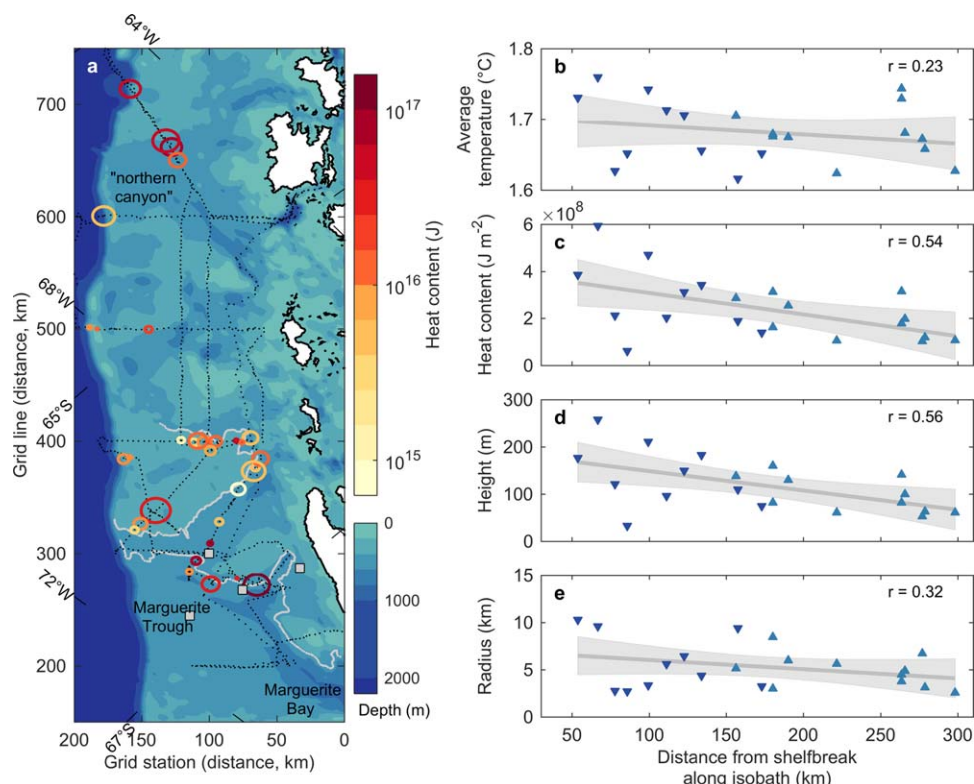


Figure 4. (a) Map of WAP continental shelf with overlaid eddies detected by the gliders, colored by the average heat content of the profiles measured within them. Dotted black lines show glider tracks. Gray squares show the locations of SO GLOBEC moorings [Moffat *et al.*, 2009] and LTER [Martinson and McKee, 2012] moorings that have been used in previous studies to measure frequency of eddy intrusion into Marguerite Bay. Gray lines trace the (top) 400 m and (bottom) 500 m bathymetric contours representing “upper” and “lower” paths of Marguerite Trough. Dark blue downward-pointing triangles in Figures 4b–4e show data from eddies lying along lower contour, and light blue upward-pointing triangles show data from eddies lying along upper contour. Gray lines and shading in Figures 4b–4e represent least squares fit to data and 95% confidence bounds. Correlation coefficients are given.

or as isolated profiles near the locations where eddies were found, which may represent remnants of larger features that had dissipated or instances of interleaving.

Mooring observations from the vicinity of Marguerite Trough previously identified eddies there [Moffat *et al.*, 2009; Martinson and McKee, 2012]. Glider observations confirm that this canyon is important for the advection of eddies onto the shelf and identify an additional, previously undetected, intrusion pathway to the north. The “northern canyon” (Figure 4a) is a cross-shelf canyon that lies outside the boundaries of the LTER grid, so no observations of UCDW had been made there in LTER time series. Mesoscale features containing UCDW were found along the northern wall of this canyon. Similarly, UCDW eddies were found along the northern wall of the entrance to Marguerite Trough. Eddies that enter the shelf at Marguerite Trough appear to follow one of two pathways onto the shelf: an upper pathway follows the 400 m isobaths to the northeast and a lower pathway follows the 500 m isobaths the southeast (Figure 4a). The highest percentage of UCDW on the shelf was measured in areas with depths near 500 m (Figure 3a), which is the approximate depth of both Marguerite Trough and the northern canyon where they cross the shelf break.

3.2. Properties of UCDW Eddies

Overall, 14% of the profiles measured by the gliders on the shelf contained UCDW. Of these, 60% were contained in 33 coherent Gaussian features with properties consistent with subsurface eddies. The majority of these features were found in or around Marguerite Trough, but the northern canyon also appears to be a conduit for transport of eddies onto the shelf (Figure 3a). Fewer observations were made in that canyon than in Marguerite Trough.

The mean value of all chord lengths was 11.3 ± 5.1 km with a median value of 10.3 km. It is important to note that eddy widths measured here are an estimate of true diameters since we do not know how close

the glider came to the center or the direction of eddy travel. However, these estimates are within the range of eddy sizes predicted by the internal deformation radius [Chelton *et al.*, 1998] and are similar to the size of eddies measured by moorings on the shelf [Moffat *et al.*, 2009; Martinson and McKee, 2012].

Subsurface eddies entering the shelf contained as much as 1.93×10^{17} J of heat relative to the reference temperature (1.2°C). Eddies lose heat to the overlying winter water and to the cooler shelf waters as they are carried in the mean flow. In the general circulation pattern in the southern half of the grid, water enters onto the shelf through Marguerite Trough and makes a counter-clockwise loop following the northern branch of the canyon [Smith *et al.*, 1999; Dinniman and Klinck, 2004; Savidge and Amft, 2009]. A second branch carries water into Marguerite Bay via the southern branch of the canyon [Klinck *et al.*, 2004]. The properties of eddies detected by the gliders are consistent with this pattern.

In Figure 4, plots b–e show properties of eddies that enter Marguerite Trough as a function of distance from the shelf break along one of two isobaths. Heat content per unit area and height are most strongly correlated with distance. Eddy height is defined as the vertical distance separating the shallowest and deepest observations of UCDW within the eddy. Radius and average temperature are weakly correlated with distance. Again, the interpretation of these relationships must include a consideration of the chord-length sampling error. An eddy that a glider passed through the edge of would appear to have a shorter radius and a cooler average temperature than if the eddy had been sampled through the middle. The observations suggest that subsurface eddies enter onto the shelf with widths on the order of 10 km and are modified as they travel along an isobaths. They dissipate most of their heat vertically and less of it laterally. Slower rates of lateral diffusion and the resulting effects of lateral spreading may explain the weak correlation between eddy width and distance traveled.

3.3. Heat Balance on the WAP

A simple two-dimensional heat budget was constructed for the region of the WAP shelf where glider and CTD observations were made (Figure 5). This region extends 500 km along the coast and 100 km across the continental shelf (Figure 1a). Vertical limits are between the depth of the permanent pycnocline, which has an average depth of 160 m and generally corresponds to the $1027.63 \text{ kg m}^{-3}$ isopycnal, and the seafloor, which are separated by an average distance of 280 m. The height of the heat budget box is defined as this average distance. Following the assumption of Klinck *et al.* [2004], we assume the alongshore advection is

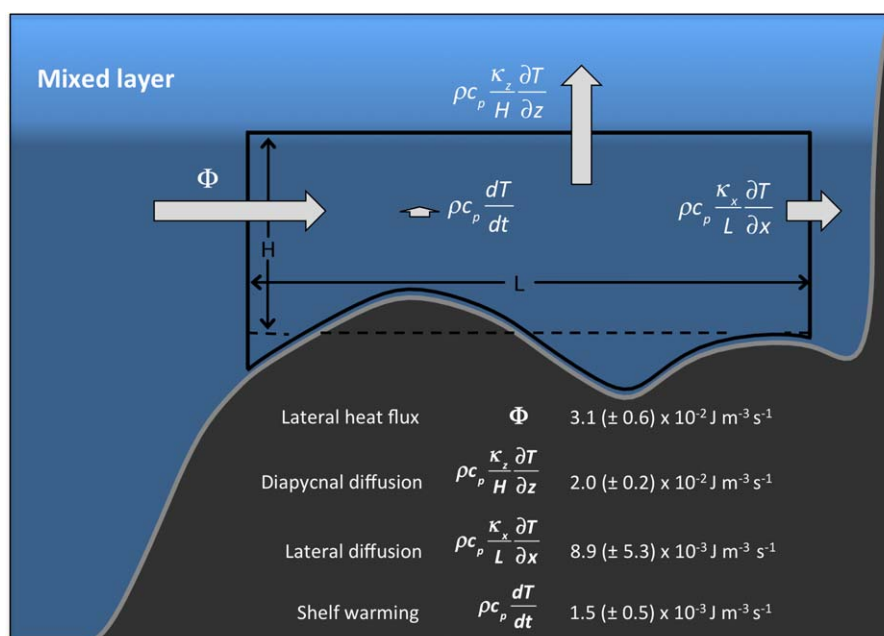


Figure 5. Schematic illustrating the components of the heat budget on the WAP continental shelf. Values shown are calculated using $\kappa_x = 100 \text{ m}^2 \text{ s}^{-1}$. All other values are listed in Table 1. We use the average bottom depth of the WAP, indicated by the dashed line, as height, H . Arrow lengths are proportional to the relative contributions of each term to the heat budget.

Table 1. Coefficients and Variables Used Throughout the Text

Symbol	Description	Value
T_{ref}	Reference seawater temperature	1.2°C
ρ	Reference seawater density	1027.7 kg m ⁻³
c_p	Specific heat of seawater	4000 J kg ⁻¹ °C ⁻¹
H	Height of heat budget box	280 m
L	Across-shelf extent of heat budget box	100 km
W	Along-shelf extent of heat budget box	500 km
κ_z	Vertical diffusivity	10 ⁻⁴ m ² s ⁻¹
κ_x	Lateral diffusivity	100 (37,200) m ² s ⁻¹
$\frac{\partial T}{\partial t}$	Time rate of change of shelf temperature	3.61 (±1.15) × 10 ⁻¹⁰ °C s ⁻¹
$\frac{\partial T}{\partial x}$	Midshelf to inner-shelf temperature gradient	2.18 (±1.28) × 10 ⁻⁶ °C m ⁻¹
$\frac{\partial T}{\partial z}$	Diapycnal temperature gradient	0.014 ± 0.002°C m ⁻¹

small and that there is no heat flux at the bottom or directly at the coast, although we do calculate lateral diffusion between the midshelf and nearshore stations. The heat balance below the permanent pycnocline on the shelf is the sum of lateral fluxes across the shelf break, diapycnal diffusion into the overlying winter water, and isopycnal diffusion across the shoreward box boundary (Figure 1a). Here we extend the analysis to include all years between 1993 and 2008, during which the overall heat content of the shelf increased [Martinson *et al.*, 2008]. Therefore, we also include a shelf warming term. Temperatures below the permanent pycnocline on the WAP shelf during the 1993–2008 sampling period warmed at an average rate of 0.01°C per year.

We integrate the advection-diffusion equation over the width (L) and depth (H) of the shelf, ignoring vertical advection and including a warming trend. We then divide by the width and depth to arrive at the volume-averaged heat budget equation:

$$\Phi - \rho c_p \left(\frac{\kappa_z}{H} \frac{\partial T}{\partial z} + \frac{\kappa_x}{L} \frac{\partial T}{\partial x} \right) = \rho c_p \frac{dT}{dt} \tag{3}$$

The lateral temperature gradient, $\frac{\partial T}{\partial x}$ is the time series average gradient of temperatures between midshelf and inner-shelf stations. Similarly, $\frac{\partial T}{\partial z}$ is the shelf-wide time-averaged temperature gradient across the permanent pycnocline at each station. H is the average vertical distance between the permanent pycnocline and the seafloor and Φ is the total flux across the shelf break. Values for all heat budget terms are listed in Table 1.

Values for the lateral and vertical diffusivities, κ_x and κ_z , respectively, are taken from the literature. Howard *et al.* [2004] estimated a shelf-wide average diapycnal diffusivity of 10⁻⁵ m² s⁻¹ based on fall and winter cruises in 2001, however this value is thought to underestimate the true mixing on the shelf which is dominated by isolated wind events [Howard *et al.*, 2004]. Estimates based on shelf-wide budgets suggest a value closer to 10⁻⁴ m² s⁻¹ [Klinck, 1998; Smith *et al.*, 1999; Smith and Klinck, 2002; Martinson *et al.*, 2008] and not exceeding 7.7 × 10⁻⁴ m² s⁻¹ [Klinck *et al.*, 2004]. As the shelf waters have warmed, the magnitude of κ_z has decreased [Martinson *et al.*, 2008]. We use 10⁻⁴ m² s⁻¹ as an average value for the shelf over the time series, which leads to an appropriate eddy-decay time scale of eddies advected with the mean flow in Marguerite Trough [Moffat *et al.*, 2009]. Estimates of isopycnal diffusivity on the shelf range from 37 m² s⁻¹ [Klinck, 1998] to 200 m² s⁻¹ [Smith *et al.*, 1999] to an unrealistic maximum of 1600 m² s⁻¹ [Klinck *et al.*, 2004]. According to mixing length arguments, lateral diffusivity scales as $\kappa \propto l$ [Prandtl, 1925]. Using a typical subpycnocline current speed of 1–5 cm s⁻¹ [Howard *et al.*, 2004; Klinck *et al.*, 2004] and a typical eddy width of 10 km, mixing length arguments indicate that lateral diffusivity should be on the order of 100–500 m² s⁻¹. This gives us confidence to use the 37–200 m² s⁻¹ range in our calculations.

Using values listed in Table 1, we calculate the average diapycnal diffusion across the permanent pycnocline, the average lateral diffusion across the inner heat box boundary, and the rate of shelf warming over the 1993–2008 shipboard sampling period. The magnitude of diapycnal diffusion is about twice that of lateral diffusion and the shelf warming term is, comparatively, very small. Of the heat that enters the shelf below the permanent pycnocline, approximately two-thirds is diffused vertically across the permanent pycnocline and one-third reaches the coastal waters by lateral diffusion.

We calculate the horizontal lateral flux, Φ , required to balance the other terms, to be $1.36 \times 10^{19} \text{ J yr}^{-1}$ (ranging from 0.97×10^{19} to $2.23 \times 10^{19} \text{ J yr}^{-1}$ depending on the lateral diffusivity, and including error estimates). This value is found by multiplying Φ in equation (3) by the volume of the heat budget box, and represents the total lateral heat flux from various mechanisms, including eddies transported onto the shelf. The average heat content of eddies observed near the shelf break is $5.8 \times 10^{16} \text{ J}$. The total annual heat flux onto the shelf is equivalent to 150–342 eddies with an average temperature of 1.7°C across a diameter of 12 km (the average temperature and width of observed eddies within 50 km of the shelf break) coming onto the shelf each year.

Year-round mooring observations at a fixed location north of Marguerite Trough led to estimates that 35–40 eddies containing UCDW passed by the mooring location each year during 2007, 2008, and 2010 [Martinson and McKee, 2012]. Observations from a mooring shoreward of that location, within the trough itself, showed similar numbers of eddies passing there [Moffat et al., 2009]. Our results show that eddies occur at similar densities to the north and south of the Marguerite Trough entrance so, assuming the trough is a conduit for 70–80 eddies per year, it alone could serve as the entryway for 20–53% of the necessary heat flux to the shelf. The northern canyon appears to be an additional location of eddy intrusion, although further observations there will be necessary to quantify its contribution as an eddy delivery pathway. In 186 days on the shelf, our gliders encountered 33 eddies suggesting that a lower-limit estimate of eddy intrusions onto the WAP shelf each year is around 64, which would account for 19–43% of the range of lateral heat flux estimates.

4. Conclusions

High-resolution measurements from Slocum Webb deep gliders deployed along the west Antarctic Peninsula confirm that warm water from the ACC is intruding onto the continental shelf as distinct mesoscale features [Moffat et al., 2009; Martinson and McKee, 2012; St-Laurent et al., 2013; Graham et al., 2016]. The high-spatial resolution of the glider data allows us to present the first near-synoptic cross sections of mesoscale eddies on the WAP. We estimate the eddy-like boluses to be on the order of 10 km wide and 125 m thick. Intrusions tend to occur at Marguerite Trough and a second cross-shelf canyon in the northern part of the study area. The annual shipboard CTD measurements also indicate these two canyons act as primary conduits for heat transport, but they are unable to resolve the spatial extent of the intrusions.

Glider measurements have allowed us to capture warm water features over a larger area of the WAP continental shelf than was previously available, but we still lack information about the mechanism by which the warm deep water, once on the shelf, reaches the coastal surface waters. Recent research using gliders suggests that bathymetry plays an important role in local mixing of deep and surface waters and may be important in the transformation of water masses across the entire shelf [Venables et al., 2016]. Melting of the glaciers on the West Antarctic Peninsula could raise global sea levels by up to $69 \pm 5 \text{ mm}$ [Huss and Fari-notti, 2014] and most of the glacier retreat since the 1990s can be attributed to interactions with the ocean [Cook et al., 2016]. Understanding the rate at which heat contained in the ocean is melting the ice is crucial to predicting how much ice will be lost in the warming climate. The UCDW features described here may account for up to 50% of the onshore heat flux, with the remainder likely to come from upwelling and advection of the ACC onto the shelf. Future efforts will focus on a better understanding of the eddy dissipation processes and the mechanisms responsible for bringing the remaining heat to the shelf.

References

- Bower, A. S., R. M. Hendry, D. E. Amrhein, and J. M. Lilly (2013), Direct observations of formation and propagation of subpolar eddies into the Subtropical North Atlantic, *Deep Sea Res., Part II*, 85, 15–41, doi:10.1016/j.dsr2.2012.07.029.
- Bromwich, D. H., J. P. Nicolas, A. J. Monaghan, M. A. Lazzara, L. M. Keller, G. A. Weidner, and A. B. Wilson (2013), Central West Antarctica among the most rapidly warming regions on Earth, *Nat. Geosci.*, 6, 139–145.
- Chelton, D. B., R. A. deSzoeke, M. G. Schlax, K. El Naggar, N. Siwertz, D. B. Chelton, R. A. deSzoeke, M. G. Schlax, K. El Naggar, and N. Siwertz (1998), Geographical variability of the first baroclinic Rossby radius of deformation, *J. Phys. Oceanogr.*, 28(3), 433–460, doi:10.1175/1520-0485(1998)028<0433:GVOTFB>2.0.CO;2.
- Cook, A. J., A. J. Fox, D. G. Vaughan, and J. G. Ferrigno (2005), Retreating Glacier Fronts on the Antarctic Peninsula over the Past Half-Century, *Science*, 308(5721), 541–544, doi:10.1126/science.1104235.
- Cook, A. J., P. R. Holland, M. P. Meredith, T. Murray, A. Luckman, and D. G. Vaughan (2016), Ocean forcing of glacier retreat in the western Antarctic Peninsula, *Science*, 353(6296), 283–286, doi:10.1126/science.aae0017.

Acknowledgments

Glider data used in this study are available through the Rutgers University Center for Ocean Observing Leadership (RUCOOL) webpage <http://marine.rutgers.edu/cool/auvs/> and the MARACOOS assets page <http://maracoos.org/data>. Data sets are also available upon request to ncouto@marine.rutgers.edu. We gratefully acknowledge support from the National Science Foundation (NSF/PLR Award 0823101), from Teledyne Webb Research for providing graduate student funding and from the RUCOOL glider technicians and pilots for their tireless work during deployments. We would also like to thank Darren McKee for several productive conversations and our anonymous reviewers for their careful criticism that helped to improve the manuscript.

- Davis, R. E., C. C. Eriksen, and C. P. Jones (2002), Autonomous buoyancy-driven underwater gliders, in *The Technology and Applications of Autonomous Underwater Vehicles*, edited by G. Griffiths, pp. 37–58, Taylor and Francis, London.
- Dinniman, M. S., and J. M. Klinck (2004), A model study of circulation and cross-shelf exchange on the west Antarctic Peninsula continental shelf, *Deep Sea Res., Part II*, 51, 2003–2022.
- Dinniman, M. S., J. M. Klinck, and W. O. Smith Jr. (2011), A model study of Circumpolar Deep Water on the West Antarctic Peninsula and Ross Sea continental shelves, *Deep Sea Res., Part II*, 58(13–16), 1508–1523, doi:10.1016/j.dsr2.2010.11.013.
- Ducklow, H., et al. (2012), The marine system of the Western Antarctic Peninsula, in *Antarctic Ecosystems an Extreme Environment in a Changing World*, edited by A. D. Rogers et al., Blackwell, London.
- Erickson, Z. K., A. F. Thompson, N. Cassar, J. Sprintall, and M. R. Mazloff (2016), An advective mechanism for deep chlorophyll maxima formation in southern Drake Passage, *Geophys. Res. Lett.*, 43, 10,846–10,855, doi:10.1002/2016GL070565.
- Graham, J. A., M. S. Dinniman, and J. M. Klinck (2016), Impact of model resolution for on-shelf heat transport along the West Antarctic Peninsula, *J. Geophys. Res. Oceans*, 121, 7880–7897, doi:10.1002/2016JC011875.
- Heywood, K. J., et al. (2014), Ocean processes at the Antarctic continental slope, *Philos. Trans. R. Soc. A*, 372(2019), 20130047, doi:10.1098/rsta.2013.0047.
- Hofmann, E. E., J. M. Klinck, C. M. Lascara, and D. A. Smith (1996), Water mass distribution and circulation west of the Antarctic Peninsula and including Bransfield Strait, in *Foundations for Ecological Research West of the Antarctic Peninsula*, edited by R. M. Ross, E. E. Hofmann, and L. B. Quentin, pp. 61–80, AGU, Washington, D. C.
- Howard, S. L., J. Hyatt, and L. Padman (2004), Mixing in the pycnocline over the western Antarctic Peninsula shelf during Southern Ocean GLOBEC, *Deep Sea Res., Part II*, 51(17–19), 1965–1979, doi:10.1016/j.dsr2.2004.08.002.
- Huss, M., and D. Farinotti (2014), A high-resolution bedrock map for the Antarctic Peninsula, *The Cryosphere*, 8, 1261–1273.
- Jenkins, A., P. Dutrieux, S. S. Jacobs, S. D. McPhail, J. R. Perrett, A. T. Webb, and D. White (2010), Observations beneath Pine Island Glacier in West Antarctica and implications for its retreat, *Nat. Geosci.*, 3(7), 468–472, doi:10.1038/ngeo890.
- Klinck, J. M. (1998), Heat and salt changes on the continental shelf west of the Antarctic Peninsula between January 1993 and January 1994, *J. Geophys. Res.*, 103, 7617–7636, doi:10.1029/98JC00369.
- Klinck, J. M., and M. S. Dinniman (2010), Exchange across the shelf break at high southern latitudes, *Ocean Sci. Discuss.*, 6, 513–524, doi:10.5194/os-6-513-2010.
- Klinck, J. M., E. E. Hofmann, R. C. Beardsley, B. Salihoglu, and S. Howard (2004), Water-mass properties and circulation on the west Antarctic Peninsula Continental Shelf in Austral Fall and Winter 2001, *Deep Sea Res., Part II*, 51, 1925–1946, doi:10.1016/j.dsr2.2004.08.001.
- Martinson, D. G., and D. C. McKee (2012), Transport of warm Upper Circumpolar Deep Water onto the western Antarctic Peninsula continental shelf, *Ocean Sci. Discuss.*, 8, 433–442, doi:10.5194/os-8-433-2012.
- Martinson, D. G., S. E. Stammerjohn, R. A. Iannuzzi, R. C. Smith, and M. Vernet (2008), Western Antarctic Peninsula physical oceanography and spatio-temporal variability, *Deep Sea Res., Part II*, 55(18–19), 1964–1987, doi:10.1016/j.dsr2.2008.04.038.
- Meredith, M. P., and J. C. King (2005), Rapid climate change in the ocean west of the Antarctic Peninsula during the second half of the 20th century, *Geophys. Res. Lett.*, 32, L19604, doi:10.1029/2005GL024042.
- Moffat, C., B. Owens, and R. C. Beardsley (2009), On the characteristics of Circumpolar Deep Water intrusions to the west Antarctic Peninsula Continental Shelf, *J. Geophys. Res.*, 114, C05017, doi:10.1029/2008JC004955.
- Pelland, N. A., C. C. Eriksen, and C. M. Lee (2013), Subthermocline Eddies over the Washington Continental Slope as Observed by Sea-gliders, 2003–09, *J. Phys. Oceanogr.*, 43, 2025–2053, doi:10.1175/JPO-D-12-086.1.
- Prandtl, L. (1925), Bericht über Untersuchungen zur ausgebildeten Turbulenz, *Z. Angew. Math. Mech.*, 5(2), 136–139.
- Prézelin, B. B., E. E. Hofmann, C. Mengelt, and J. M. Klinck (2000), The linkage between Upper Circumpolar Deep Water (UCDW) and phytoplankton assemblages on the west Antarctic Peninsula continental shelf, *J. Mar. Res.*, 58, 165–202.
- Prézelin, B. B., E. E. Hofmann, M. Moline, and J. M. Klinck (2004), Physical forcing of phytoplankton community structure and primary production in continental shelf waters of the Western Antarctic Peninsula, *J. Mar. Res.*, 62(3), 419–460, doi:10.1357/0022240041446173.
- Pritchard, H. D., S. R. M. Ligtenberg, H. A. Fricker, D. G. Vaughan, M. R. van den Broeke, and L. Padman (2012), Antarctic ice-sheet loss driven by basal melting of ice shelves, *Nature*, 484, 502–505, doi:10.1038/nature10968.
- Rignot, E., and S. S. Jacobs (2002), Rapid bottom melting widespread near Antarctic ice sheet grounding lines, *Science*, 296(5575), 2020–2023, doi:10.1126/science.1070942.
- Rignot, E., J. Mouginot, M. Morlighem, H. Seroussi, and B. Scheuchi (2014), Widespread, rapid grounding line retreat of Pine Island, Thwaites, Smith, and Kohler glaciers, West Antarctica, from 1992 to 2011, *Geophys. Res. Lett.*, 41, 3502–3509, doi:10.1029/2011GL046583.
- Savidge, D. K., and J. A. Amft (2009), Circulation on the West Antarctic Peninsula derived from 6 years of shipboard ADCP transects, *Deep Sea Res., Part I*, 56(10), 1633–1655, doi:10.1016/j.dsr.2009.05.011.
- Schmidtke, S., K. J. Heywood, A. F. Thompson, and S. Aoki (2014), Multidecadal warming of Antarctic waters, *Science*, 346, 1227–1231, doi:10.1126/science.1256117.
- Schofield, O., et al. (2007), Slocum Gliders: Robust and ready, *J. Field Robotics*, 24(6), 473–485, doi:10.1002/rob.20200.
- Smith, D. A., and J. M. Klinck (2002), Water properties on the west Antarctic Peninsula continental shelf: A model study of effects of surface fluxes and sea ice, *Deep Sea Res., Part II*, 49, 4863–4886, doi:10.1016/S0967-0645(02)00163-7.
- Smith, D. A., E. E. Hofmann, J. M. Klinck, and C. M. Lascara (1999), Hydrography and circulation of the West Antarctic Peninsula Continental Shelf, *Deep Sea Res., Part I*, 46, 925–949.
- Smith, R. C., et al. (1995), The Palmer LTER: A long-term ecological research program at Palmer Station, Antarctica, *Oceanography*, 8, 77–86.
- St-Laurent, P., J. M. Klinck, and M. S. Dinniman (2013), On the role of coastal troughs in the circulation of warm Circumpolar Deep Water on Antarctic shelves, *J. Phys. Oceanogr.*, 43, 51–64, doi:10.1175/JPO-D-11-0237.1.
- Turner, J., T. A. Lachlan-Cope, S. Colwell, G. J. Marshall, and W. M. Connolley (2006), Significant warming of the Antarctic winter troposphere, *Science*, 311, 1914–1917, doi:10.1126/science.1121652.
- Turner, J., H. Lu, I. White, J. C. King, T. Phillips, J. S. Hosking, T. J. Bracegirdle, G. J. Marshall, R. Mulvaney, and P. Deb (2016), Absence of 21st century warming on Antarctic Peninsula consistent with natural variability, *Nature*, 535(7612), 411–415, doi:10.1038/nature18645.
- Venables, H. J., M. P. Meredith, and J. A. Brearley (2016), Modification of deep waters in Marguerite Bay, western Antarctic Peninsula, caused by topographic overflows, *Deep Sea Res., Part II*, doi:10.1016/j.dsr2.2016.09.005.
- Zhang, Z., P. Li, L. Xu, C. Li, W. Zhao, J. Tian, and T. Qu (2015), Subthermocline eddies observed by rapid-sampling Argo floats in the subtropical northwestern Pacific Ocean in Spring 2014, *Geophys. Res. Lett.*, 42, 6438–6445, doi:10.1002/2015GL064601.